Blastocyst formation rate depends on oxygen consumption rates.

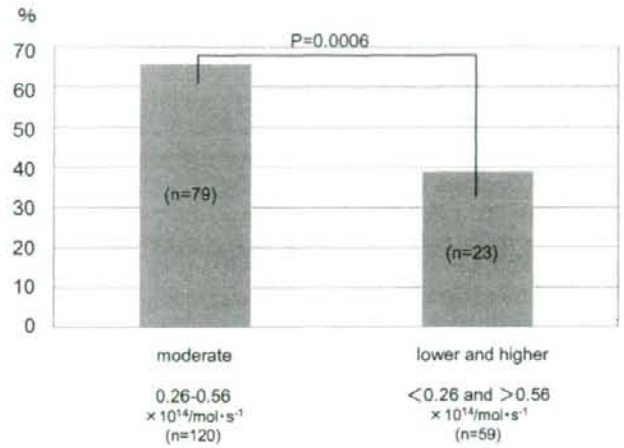

Fig. 3. Embryos with moderate respiration rates showed high developmental rate (65.8%) to the blastocyst. The developmental rate of embryos with lower and higher respiration rates was 39.0%.

Blastocyst formation rate after measurement of oxygen consumption.

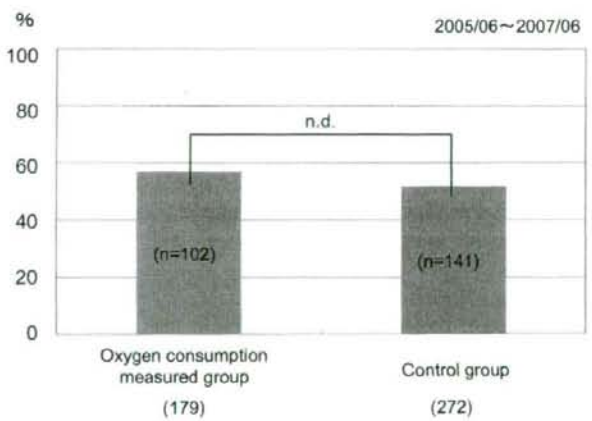

Fig. 4. The safety of SECM is assured as the embryos which were examined by SECM for oxygen consumption showed the same levels of development as the control group.

blastocysts and for implantation [3]. A report on the correlation between pronuclear pattern and pregnancy rate suggested that groups with particular pronuclear patterns tend to provide good results in pregnancy [4].

Morphological evaluation has been widely performed to assess embryo quality because it is non-invasive and useful in predicting pregnancy rate. Morphological observations have contributed significantly to the great success of ART programs in humans. In some cases, however, even embryos with low quality result in

successful pregnancy, whereas many good embryos, as judged by morphological observation, fail to result in pregnancy. Furthermore, morphological evaluation remains one of the most subjective and least quantitative aspects of embryo transfer, because categorization standards vary among the investigators. Recently, a very interesting study used time-lapse cinematography to morphologically analyze human embryonic development [5]. Numerous excellent findings by this method indicate that the dynamic observation of human gametes during the early stages of embryo development are of paramount interest for clarifying the physiological events during the fertilization process. The authors of that study suggested that there may be some limitations in momentary morphological observations of embryos which are dynamically changing [5].

The blastocyst stage transfer was proposed so that embryos could be evaluated, and some clinicians perform day 5 embryo transfer, even now. The principle idea is that, *in vivo*, cleavage stage embryos reside in the Fallopian tube and not in the uterus. The potential advantages of blastocyst culture and transfer include the synchronization of the embryo with the female tract leading to increased implantation rate and assessment of viability of an embryo before transfer [6]. The theory is sound and acceptable. The results of prospective randomized studies, however, clearly show that there is no advantage of the blastocyst stage transfer over the conventional cleavage stage transfer [7, 8].

Other new methods are needed in ART, especially selection methods to obtain the best quality embryos. Fundamentally, in embryos, the maturation of mitochondria is associated with increases in metabolism reflected by their oxygen consumption and CO_2 production [9]. So, mitochondrial function (oxygen consumption) may be an important parameter of embryo quality [9]. It is well known that metabolic processes change during embryonic development, as indicated by genome activation and large increases in protein synthesis. Oxygen consumption is a parameter used to gain valuable information on metabolic mechanisms. Oxygen consumption of mammalian embryos has been studied with various methods such as Cartesin a diver [9], spectrophotometrics [10–12], fluorescence [13–15] and electrochemical techniques [16–20].

The measurement of oxygen respiration rate (oxygen consumption) of bovine embryos has been employed to investigate the correlation between respiration rate and embryo morphology, diameter and sex, and it has been shown that the respiration rate is directly influenced by embryo diameter but does not differ between sexes [21]. So, respiration rates are only in partial agreement with embryo morphology, suggesting a slight discrepancy between these two methods of assessing embryo quality, and it is likely that a combined assessment of embryo respiration rate and morphology would improve embryo classification and subsequent selection.

The accuracy and simplicity of a measuring method is an essential and important point. With regard to this, the methods for measuring respiration rate for single bovine embryos were reported [22, 23]. The respiration activity of single bovine embryos entrapped in a cone-shaped microwell was monitored by scanning electrochemical microscopy. Using this method, the results for oxygen consumption rates of embryos of rank A (very good) were significantly higher than those of rank B (good). Furthermore, there were no apparent differences of oxygen consumption rate between male and female embryos [24]. These results indicate that the oxygen consumption rate of individual embryos reflects their quality but does not correlate with the sex ratio of embryos with excellent quality.

From the results of the present study, we deduce the following: 1) embryos have different oxygen consumption rates, even among morphologically similar embryos; 2) there is no correlation between morphological quality and respiration activity in human embryos at the early developmental stage; and 3) embryos with moderate respiration rates have better potential for further development than those with lower and higher respiration rates.

Conclusion

SECM can be used to measure the oxygen consumption of single human embryos at various developmental stages. The maturation of mitochondria correlates with the increase in oxygen consumption during the development of embryos. The development of mitochondria may be an important factor of embryo quality, because mitochondria provide ATP for embryonic development by metabolism of nutrients in the cytoplasm. The SECM technique may be a valuable tool for accurately assessing mitochondrial function and the quality of human embryos.

There was no correlation between morphological quality and respiration activity in human embryos at the early developmental stage. Embryos with moderate respiration rates had better potential for further

development than those with lower or higher respiration rates. The present results support the hypothesis that measuring embryonic respiration provides additional and valuable information about embryo quality.

References

1) Abe, H., Shiku, H., Aoyagi, S., Matsue, T. and Hoshi, H. (2005): Respiration activity of bovine embryos cultured in serum-free and serum-containing media. Reprod. Fertil. Develop., 17, 205.
2) Abe, H. (2007): A non-invasive and sensitive method for measuring cellular respiration with a scanningn electrochemical microscopy to evaluate embryo quality. J. Mamm. Ova. Res., 24, 70–78.
3) Ebner, T., Moser, M., Sommergruber, M., Yaman, C., Pfleger, U. and Tews, G. (2002): First polar body morphology and blastocyst formation rate in ICSI patients. Hum. Reprod., 9, 2415–2418.
4) Tesarik, J., Junca, A.M., Hazout, A., Aubriot, F.X., Nathan, C., Cohen-Bacrie, P. and Dumont-Hassan, M. (2000): Embryos with high implantation potential after intracytoplasmic sperm injection can be recognized by a simple, non-invasive examination of pronuclear morphology. Hum. Reprod., 6, 1396–1399.
5) Mio, Y. (2006): Morphological analysis of human embryonic development using time-lapse cinematography. J. Mamm. Ova Res., 23, 27–35.
6) Gardner, D.K., Schoolcraft, W.B., Wagley, L., Schlenker, T., Stevens, J. and Hesla, J. (1998): A prospective randomized trial of blastocyst culture and transfer in in-vitro fertilization. Hum. Reprod., 12, 3434–3440.
7) Utsunomiya, T., Naitou, T. and Nagaki, M. (2002): A prospective trial of blastocyst culture and transfer. Hum. Reprod., 7, 1846–1851.
8) Utsunomiya, T., Ito, H., Nagaki, M. and Sato, J. (2004): A prospective, randomized study: day 3 versus hatching blastocyst stage. Hum. Reprod., 7, 1598–1603.
9) Mills, R.M. and Brinster, R.L. (1967): Oxygen consumption of preimplantation mouse embryos. Exp. Cell. Res., 47, 337–344.
10) Magnusson, C., Hillensjo, T., Hamberger, L. and Nilsson, L. (1986): Oxygen consumption by human oocytes and blastocysts grown in vitro. Hum. Reprod., 1, 183–184.
11) Magnusson, C., Hillensjo, T., Tsafriri, A., Hultborn, R. and Ahren, K. (1977): Oxygen consumption of maturing rat oocytes. Biol. Reprod., 17, 9–15.
12) Nilsson, B., Magnusson, C., Widehn, S. and Hillensjo, T. (1982): Correlation between blastocyst oxygen consumption and trophoblast cytochrome oxidase reaction at initation of implantation of delayed mouse blastocysts. J. Embryol. Exp. Morphol., 71, 75–82.
13) Houghton, F.D., Thompson, J.G., Kennedy, C.J. and Leese, H.J. (1996): Oxygen consumption and energy metabolism of the early mouse embryo. Mol. Reprod. Dev., 44, 476–485.
14) Thompson, J.G., Partridge, R.J., Houghton, F.D., Cox, C.I. and Leese, H.J. (1996): Oxygen uptake and carbohydrate metabolism by in vitro derived bovine embryos. J. Reprod. Fertil., 106, 299–306.
15) Donnay, I. and Leese, H.J. (1999): Embryo metabolism during the expansion of the bovine blastocyst. Mol. Reprod. Dev., 53, 171–178.
16) Overstrom, E.W., Duby, R.T., Dobrinsky, J., Roche, J.F. and Boland, M.P. (1992): Viability and oxidative metabolism of the bovine blastocyst. Theriogenology, 37, 269.
17) Smith, P.J.S., Hammar, K., Porterfield, D.M., Sanger, R.H. and Trimarchi, J.R. (1999): Self-referencing, non-invasive, ion selective electrode for single cell detection of transplasma membrane calcium flux. Microsc. Res. Tech., 46, 398–417.
18) Land, S.C., Porterfield, D.M., Sanger, R.H. and Smith, P.J.S. (1999): The self-referencing oxygen-selective microelectrode: detection of transmembrane oxygen flux from single cells. J. Exp. Biol., 202, 211–218.
19) Porterfield, D.M., Trimarchi, J.R., Keefe, D.L. and Smith, P.J.S. (1998): Characterization of oxygen and calcium fluxes from early mouse embryos and oocytes. Biol. Bull., 195, 208–209.
20) Trimarchi, J.R., Liu, L., Porterfield, D.M., Smith, P.J.S. and Keefe, D.L. (2000): Oxidative phosphorylation-dependent and -independent oxygen consumption by individual preimplantation mouse embryos. Biol. Reprod., 62, 1866–1874.
21) Lopes, A.S., Larsen, L.H., Ramsing, N., Løvendahl, P., Raty, M., Peippo, J., Greve, T. and Callesen, H. (2005): Respiration rates of individual bovine in vitro-produced embryos measured with a novel, non-invasive and highly sensitive microsensor system. Soc. Reprod. Fertil., ISSN 1470–1626 (paper), 1741–7899 (online).
22) Shiku, H., Shiraishi, T., Ohya, H., Matsue, T., Abe, H., Hoshi, H. and Kobayashi, M. (2001): Oxygen consumption of single bovine embryos probed by scanning electrochemical microscopy. Anal. Chem., 73, 3751–3758.
23) Shiku, H., Shiraishi, T., Aoyagi, S., Utsumi, Y., Matsudaira, M., Abe, H., Hoshi, H., Kasai, S., Ohya, H. and Matsue, T. (2004): Respiration activity of single bovine embryos entrapped in a cone-shaped microwell monitored by scanning electrochemical microscopy. Anal. Chimica. Acta, 522, 51–58.
24) Agung, B., Otoi, T., Abe, H., Hoshi, H., Murakami, M., Karja, N.W.K., Murakami, M.K., Wongsrikeao, P., Watari, H. and Suzuki, T. (2005): Relationship between oxygen consumption and sex of bovine in vitro fertilized embryos. Reprod. Dom. Anim., 40, 51–56.

Transactions of the Materials Research Society of Japan 33[3] 759-762 (2008)

Measurement of the Respiratory Activity of Single Human Embryos by Scanning Electrochemical Microscopy

Hiroyuki Abe[1*], Masaki Yokoo[2], Takahiro Itoh-Sasaki[1], Megumi Nasu[3], Kaori Goto[3], Yoko Kumasako[3], Yasuhisa Araki[4], Hitoshi Shiku[5], Tomokazu Matsue[5], Takafumi Utsunomiya[3]

[1*]Graduate Program of Human Sensing and Functional Sensor Engineering, Graduate School of Science and Engineering, Yamagata University, Yonezawa, Japan; [2]Innovation of New Biomedical Engineering Center, Tohoku University, Sendai, Japan; [3]St-Luke Clinic, Oita, Japan; [4]The Institute for ARMT, Gunma, Japan; [5]Graduate School of Environmental Studies, Tohoku University, Sendai, Japan

*To whom correspondence should be addressed Fax: 81-238-26-3361; e-mail: abeh@yz.yamagata-u.ac.jp

Respiration is useful parameter for evaluating embryo quality as it provides important information about metabolic activity. In the present study, we employed scanning electrochemical microscopy (SECM) to accurately determine the oxygen consumption of single, identical human embryos at different developmental stages. The oxygen consumption rates of single embryos were low at 2-8-cell stages ($0.51 \pm 0.05 \times 10^{14}$/mol・$s^{-1}$, n=18) but increased by the morula ($0.61 \pm 0.11 \times 10^{14}$ /mol・s^{-1}, n=5) and early blastocyst ($0.72 \pm 0.06 \times 10^{14}$/mol・$s^{-1}$, n=14) stages. Later blastocysts exhibited even higher oxygen consumption rates ($1.00 \pm 0.19 \times 10^{14}$/mol・$s^{-1}$, n=4). Ultrastructural studies revealed that most mitochondria in embryos up to the 8-cell stage were immature and had a spherical or ovoid shape. However, by the morula stage, the mitochondria had elongated cristae, with the elongated morphology even more pronounced in mitochondria present in blastocysts. The maturation of mitochondria correlated with the increase of oxygen consumption rate during the development of embryos. The SECM technique may be a valuable tool for accurately assessing the mitochondrial function and quality of human embryos.

Key words: cell respiration; electrochemical miscroscopy; human embryo; culture

INTRODUCTION

Embryo quality is an important determinant of the success of embryo transfer and accurate evaluation of embryo quality improves the pregnancy rate for assisted reproduction of mammals, including humans. Several approaches have been used to evaluate embryo quality and viability. Morphological evaluation is the primary method. However, morphological evaluation is subjective and difficult, especially for embryos with intermediate morphological qualities [1]. Therefore, more objective selection criteria are needed.

The metabolic activity of embryos has been determined from the consumption of nutrients, such as glucose, pyruvate and amino acids [2]. Oxygen consumption is an ideal indicator of overall metabolic activity because adenosine triphosphate (ATP) is generated predominantly by oxidative phosphorylation, a process in which oxygen plays an essential role [3]. In previous paper we describe a novel cell respiration measuring system, scanning electrochemical microscopy (SECM). This technique is a useful method for evaluating embryo quality that correlates metabolic respiration with morphological quality, developmental potential, and pregnancy rate following embryo transfer [4]. In this study, we employed SECM to accurately determine the oxygen consumption of single, identical human embryos at different developmental stages.

MATERIAL AND METHODS

Oocyte retrieval and embryo culture

Ovarian stimulation was performed using with human menopausal gonadotropin (HMG; Nikken Kagaku, Tokyou, Japan), gonadotropin-releaseing hormone (GnRH) agonist (Buserecur, Fujiseiyaku, Tokyo, Japan), using the extended protocol. Human chorionic gonadotropin (HCG; Profasi, Serono, Switzerland, 10,000IU) was administrated when the diameter of the dominant follicle was 20 mm. Transvaginal oocyte aspiration was performed 34 h after HCG was administrated.

Oocytes were inseminated by conventional *in vitro* fertilization

(IVF) by 3-4 h after oocyte retrieval. Following an IVF-embryo transfer (ET) procedure, surplus embryos that patients preferred not to keep preserved were designated for our study. Informed consent for use of embryos in research was obtained from all patients. The embryos were cultured in Sydney IVF Cleavage Medium (Cook IVF, Brisbane, Australia) until Day 3, after which they were cultured in Sydney IVF Blastocyst Medium (Cook IVF). Embryos were evaluated by the Veeck method [5] at early developmental stage (day 3 after IVF) and by the Gardner method [6] at blastocyst stage based on their morphological features.

Scanning electrochemical microscopy measuring system

In this study, oxygen consumption was measured by SECM procedure [7,8]. This modified SECM system includes a measuring instrument on an inverted optical microscope stage, a potentiostat (Hokuto Denko Co., Tokyo, Japan), and a notebook computer as controller and analyzer (Fig. 1a-d). Pt-microdisk electrodes sealed in a tapered soft-glass capillary (Fig. 1e) were fabricated according to the method [9]. The tip potential was held at -0.6V versus Ag/AgCl with a potentiostat to monitor the local oxygen concentration in the solution. For the measurement of oxygen consumption, HFF99 medium (Fuso Pharmaceutical Industries, Osaka, Japan) was employed. Voltammetry of the Pt-microdisk electrode in HFF99 medium showed a steady-state oxygen reduction wave. No response from other electrochemically active species was observed near the oocyte surface. The tip scanning rate was 31.1 μm/s. The microelectrode with a Pt-disk radius less than 3 μm was selected so that the oxygen reduction current of the electrode was less than 1.0 nA. To easily handle many oocytes in a short time, a plate with cone-shaped microwells was used (Fig. 1f). The single human embryo was transferred into a cone-shaped microwell filled with HFF99 medium and embryo fell to the bottom of the well and remained at the lowest point (Fig. 1g). The microelectrode was scanned according to the z-direction from side point of sample (Fig. 1g, h). The motor driven XYZ-stage was located on the microscope stage for electrode tip scanning. The XYZ stage and potentiostat were controled by computer. The oxygen consumption rate of embryos is calculated by newly designed software based on spherical diffusion theory [7]. Measurements of each embryo were performed very rapidly (within 1 min).

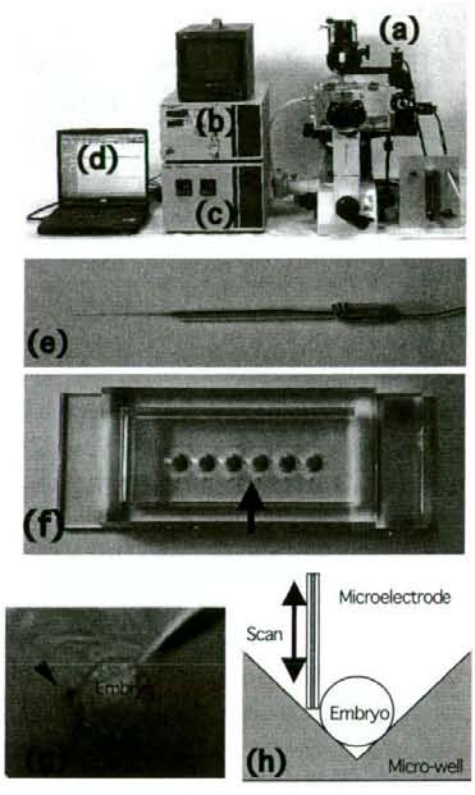

Fig. 1. A modified scanning electrochemical microscopy (SECM) system. SECM system includes a measuring instrument on the inverted optical microscope stage (a), potentiostat (b), controller (c), notebook computer (d), a microelectrode (e), and a plate (f) for measuring respiration activity of embryos. The plate has six cone-shaped microwells (arrow in f). Individual embryos are transferred into a microwell filled with medium. The embryo sinks down to the bottom of the well, remaining at the lowest point (g). Microelectrode (arrowhead in g) is scanned along the z-axis from the side point of embryo (h).

Electron microscopy

The electron microscopic study was carried out by the methods described previously [10]. Human embryos in various stages were fixed in 2.5% glutaraldehyde and postfixed in 1% osmium tetroxide in 0.1 M phosphate buffer (pH 7.4) for 1 h at 0-4 ℃. Subsequently, the embryos were individually embedded in 1% agar. All samples were dehydrated by ethanol, substituted in

propylene oxide, and embedded in epoxy resin. Ultrathin sections were cut with a diamond knife on an ultramicrotome (Reichert Ultracuts, Leica, Heerbrugg, Switzerland), stained with uranyl acetate and lead citrate, and examined using a transmission electron microscope (JEM-1210, Jeol, Tokyo, Japan).

RESULTS AND DISCUSSION

Morphology of human embryos

Figure 2 shows the morphological features of human embryos using differential interference contrast microscopy. The embryos showed various morphological features in each developmental stage. In this study, embryos classified as good quality based on their morphological features were selected and the oxygen consumption rates of individual embryos were measured by SECM system.

Oxygen consumption of human embryos in various developmental stages

Using a modified SECM measuring procedure, we successfully measured the respiration activity of single human embryos at several developmental stages (Table 1). The oxygen consumption rates of single embryos were low at 2-8-cell stages ($0.51 \pm 0.05 \times 10^{14}$/mol・$s^{-1}$, n=18) but increased by the morula ($0.61 \pm 0.11 \times 10^{14}$/mol・$s^{-1}$, n=5) and early blastocyst ($0.72 \pm 0.06 \times 10^{14}$/mol・$s^{-1}$, n=14) stages. Later blastocysts exhibited even higher oxygen consumption rates ($1.00 \pm 0.19 \times 10^{14}$/mol・$s^{-1}$, n=4). These results demonstrate that SECM can detect differences in respiration activity of human embryos at several developmental stages.

The SECM system used in the present study can detect the oxygen concentration (ΔC) as small as a 1 μM difference between the bulk solution and the embryo surface: therefore, the system gives a precise and quantitative feature of oxygen consumption of single embryo [7]. Recently, SECM has been employed to quantify the respiration activity of embryos in several animal species [11]. SECM has been utilized to measure the respiration activity of single embryos from livestock, such as cattle and pigs, as well as those from small rodents, all with high reproducibility.

Ultrasructural features of mitochondria

Ultrastructural studies revealed that most mitochondria in embryos up to the 8-cell stage are immature and have a spherical or ovoid shape (Fig. 3a). However, by the morula stage, mitochondria have elongated cristae (Fig. 3b). This morphology is even more pronounced in mitochondria present in blastocysts (Fig. 3c). These results demonstrated that the maturation of mitochondria correlates with an increase of oxygen consumption rates during the development of human embryos. Similar findings have been reported in bovine embryos [4]. Mitochondria exhibited specific morphological changes as the respiration activity increased, because the number of mitochodria per cell and the number of cristae per mitochondrion are related to the energy requirement by respiration [12].

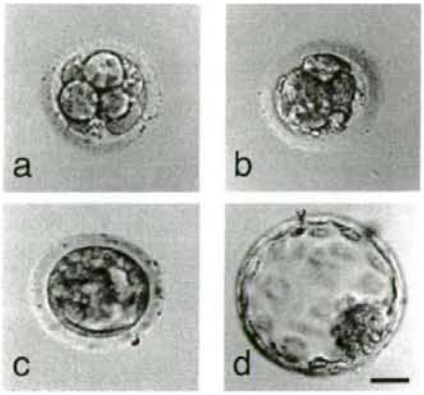

Fig. 2. Nomarski differential interference micrographs of 8-cell (a), morula (b), early blastocyst (c), and blastocyst (d) stages of human embryos developed from in vitro fertilized oocytes. Bar = 50 μm.

Table 1. Oxygen consumption rates of human embryos at various developmental stages

Embryonic stage	No. of embryos examined	O_2 consumption rate ($F \times 10^{14}$/mol・s^{-1})
2-8 cell	18	0.51 ± 0.05^{a}
Morula	5	0.61 ± 0.11^{ab}
Early blastocyst	13	0.72 ± 0.06^{b}
Blastocyst	4	1.00 ± 0.19^{c}

Values with different superscripts in each column are significantly different ($P < 0.05$).

Mitochondria contribute a vital role to the metabolism of

energy-compounds in the cytoplasm to provide ATP for embryonic development. The development of mitochondria may be an important factor in embryo quality. There are conspicuous differences in the ultrastructural features of bovine embryos of high and low quality [13]. Morulae classified as low quality by morphological classification contained nucleoli with low transcriptional activity, a large number of lipid droplets, and immature mitochondria, consistent with these low quality embryos displaying low metabolic activities, including oxygen consumption. Thus, oxygen consumption associated with mitochondrial development is a reliable indicator of embryo quality.

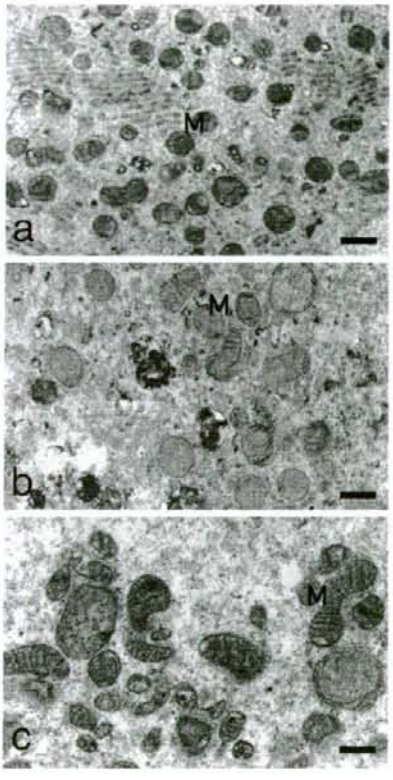

Fig. 3. Electron micrographs of human embryos at 2-cell (a), morula (b), and blastocyst (c). M, mitochondria. Bars = 0.5 μm.

CONCLUSIONS

SECM can non-invasively measure oxygen consumption by single, identical human embryos. This technique is a valuable tool for accurately assessing the mitochondrial function of human embryos. As respiration activity correlates with the quality of embryos, this technique may contribute to assessing the quality of human embryos in *in vitro* fertilization clinics.

ACKNOWLEDGEMENTS

This work was supported by Research and Development Program for New Bio-Industry Initiatives, Bio-oriented Technology Research Advancement Institution (BRAIN), Grant-in-Aid for Scientific Research (17380164), on Priority Areas "Lifesurveyor" (19021006) from the Ministry of Education, Culture, Sports, Science and Technology of Japan, Special Coordination Funds for Promoting Science and Technology of Japan, and the Japan Livestock Technology Association.

REFERENCES

[1] I. Boiso, A. Veiga, R.G. Edwards, *Reprod. Biomed. Online*, 5, 328-50 (2002).

[2] D. Rieger ,*Theriogenology*, 37, 75-93 (1992).

[3] J.R. Trimarchi, I. Liu, D.M. Porterfield, P.J.S. Smith, D.L. Keefe, *Biol. Reprod.*, 62, 1866-74 (2000).

[4] H. Abe, H. Shiku, M. Yokoo, S. Aoyagi, S. Moriyasu, A. Minamihashi, T. Matsue, H. Hoshi, *J. Reprod. Dev.*, 52 (Suppl.), S55-64 (2006).

[5] L.L. Veek, "*Atlas of the human oocyte and early conceptus*, Vol. 2. Williams & Wilkins Co, Baltimore (1991)

[6] D.K. Gardner, W.B. Scoolcraft, Jansen R., "*In vitro culture of human blastocysts*", Eds. by R. Jansen, D. Mortimer, Carnforth, Parthenon Press (1999) pp. 378-89.

[7] H. Shiku , T. Shiraishi, H. Ohya, T. Matsue, H. Abe, H. Hoshi, M. Kobayashi, *Anal. Chem.*, 73, 3751-58 (2001).

[8] H. Abe, H. Shiku, S. Aoyagi, H. Hoshi, *J. Mamm. Ova Res.*, 21, 22-30 (2004).

[9] T. Matsue, S. Koike and I. Uchida, *Biochem. Biophys. Res. Commun.*, 197, 1283-7 (1993).

[10] H. Abe, S. Yamashita, T. Satoh, H. Hoshi, *Mol. Reprod. Dev.*, 61, 57-66 (2002).

[11] H. Abe, *J. Mamm. Ova Res.*, 24, 70-78 (2007).

[12] D.W. Fawcett, Mitochondria, "*The Cell*", Philadelphia, Saunders Company (1981) pp. 410-88.

[13] H. Abe, S. Matsuzak, H. Hoshi, *Theriogenology*, 57, 1273-83 (2002).

(Recieved December 9, 2007 ; Accepted April 5, 2008)

Transactions of the Materials Research Society of Japan 33[3] 763-766 (2008)

Multiple Analysis of Respiratory Activity in the Identical Oocytes by Applying Scanning Electrochemical Microscopy

Masaki Yokoo[1], Takahiro Ito-Sasaki[2], Hitoshi Shiku[3], Tomokazu Matsue[3], Hiroyuki Abe[2*]

[1]Innovation of New Biomedical Engineering Center, Tohoku University, Sendai, Japan; [2]Graduate Program of Human Sensing and Functional Sensor Engineering, Graduate School of Science and Engineering, Yamagata University, Yonezawa, Japan; [3]Graduate School of Environmental Studies, Tohoku University, Sendai, Japan

*To whom correspondence should be addressed Fax: 81-238-26-3361; e-mail: abeh@yz.yamagata-u.ac.jp

Scanning electrochemical microscopy (SECM) is a technique in which the tip of a microelectrode is used to scan and monitor the local distribution of electro-active species near the sample surface. In this study, we have studies on the SECM technique, to establish the accurate method for measurement of respiratory activity of single pig oocytes. The oxygen consumption rates of pig oocytes cultured in modified TCM199 medium were evaluated by the SECM system. After the measuring, distribution of active mitochondria and ATP content was investigated in the identical oocytes. The oocytes were classified in three types (Type-I, Type-II or Type-III) according to the pattern of active mitochondria distribution. There was no difference in the oxygen consumption rate ($F \times 10^{14}$/mol s^{-1}) between Type-II and Type-III (0.59 and 0.60, respectively). However, the ATP content (pmol/oocyte) was significantly higher in Type-III (2.38) compared with that of Type-II (1.53). Meanwhile, the oxygen consumption rate and ATP content of Type-I were very low (0.02 and 0.06, respectively). These results suggest that the oxygen consumption rate and ATP content of oocytes was significantly affected by category of mitochondrial distribution. In the present study, we succeeded in the multiple analysis of respiratory activity in the identical oocytes. This novel system may be a valuable tool for accurately assessing the mitochondrial functions.

Key words: cell respiration; electrochemical miscroscopy; pig oocyte; culture

INTRODUCTION

Oxygen consumption is an indicator of the overall metabolic activity and quality of a single embryo. Oxygen consumption of mammalian embryos has been with various methods such as Cartesian diver [1], spectrophotometrics [2,3], fluorescence [4,5] and electrochemical techniques [6]. To establish the evaluation method for embryo quality based on the oxygen consumption activity, we have been studied on the scanning electrochemical microscopy (SECM) technique [7]. SECM technique has been successfully applied to investigate various biological systems including DNA [8], enzyme [9], antigen-antibodies [10,11], tissue [12], and cell [13], because of its non-invasive nature to quantitatively characterize localized chemical reaction under physiological conditions. In the previous study, we applied SECM technique to measure the oxygen consumption of single bovine embryos [14]. The oxygen consumption of individual bovine embryos produced in vitro fertilization (IVF) systems has been determined non-invasively and quantitatively by this technique. Furthermore, we have found that there was a close relationship between high oxygen consumption and developmental ability of bovine embryos [14-16]. The SECM procedures may be useful to assess the quality of embryos and contribute to improvements in reproductive technologies in mammals.

On the other hand, an accurate system to evaluate oocyte quality is lacking. The most convenient evaluation system for oocyte quality is based on oocyte morphology and status of oocyte-cumulus complexes (COCs). However, this evaluation method could be imprecise and subjective, since there is no clear correlation between oocyte quality and fertilization rates [17]. Oocyte quality could be one of the most important factor in determining successful fertilization and embryo development. Therefore, we attempt to establish an evaluation system for oocyte quality is based on the respiratory activity of oocytes. The aims of this study were: 1) to assess the oxygen consumption of single pig oocytes using SECM; 2) to examine the mitochondrial distribution and ATP content in the identical oocytes.

MATERIAL AND METHODS

Scanning electrochemical microscopy measuring system

In this study, oxygen consumption was measured by SECM procedure [16, 18]. This modified SECM system includes a measuring instrument on an inverted optical microscope stage, a potentiostat (Hokuto Denko Co., Tokyo, Japan), and a notebook computer as controller and analyzer (Fig. 1a-d).

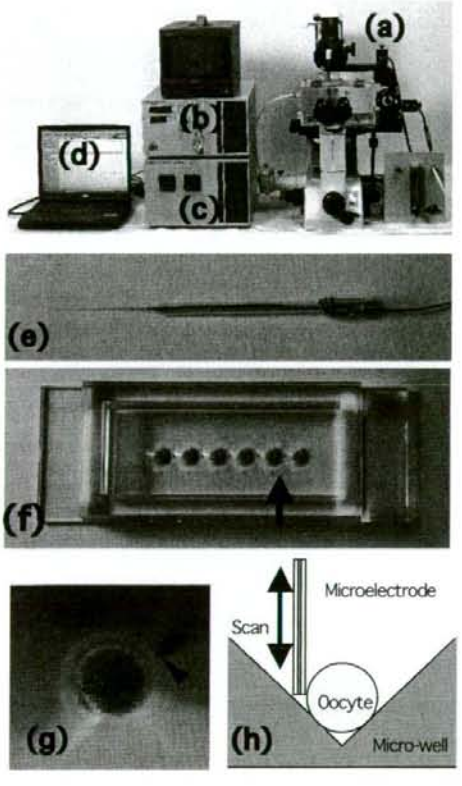

Fig. 1. A modified scanning electrochemical microscopy (SECM) system. SECM system includes a measuring instrument on the inverted optical microscope stage (a), potentiostat (b), controller (c), notebook computer (d), a microelectrode (e), and a plate (f) for measuring respiration activity of embryos. The plate has six cone-shaped microwells (arrow in f). Individual oocyte is transferred into a microwell filled with medium. The oocyte sinks down to the bottom of the well, remaining at the lowest point (g). Microelectrode (arrowhead in g) is scanned along the z-axis from the side point of oocyte (h).

Pt-microdisk electrodes sealed in a tapered soft-glass capillary were fabricated according to the method [19] (Fig. 1e). The tip potential was held at -0.6V versus Ag/AgCl with a potentiostat to monitor the local oxygen concentration in the solution. For the measurement of oxygen consumption, modified human tubal fluid (HTF) medium [20] was employed. Its composition only includes salt electrolyte, glucose, sodium pyruvate, sodium lactate, HEPES and gentamicin sulfate. Voltammetry of the Pt-microdisk electrode in modified HTF medium showed a steady-state oxygen reduction wave. No response from other electrochemically active species was observed near the oocyte surface. The tip scanning rate was 31.1 μm/s. The microelectrode with a Pt-disk radius less than 3 μm was selected so that the oxygen reduction current of the electrode was less than 1.0 nA. To easily handle many oocytes in a short time, a plate with cone-shaped microwells was used (Fig. 1f). The single pig oocyte was transferred into a cone-shaped microwell filled with modified HTF medium and oocyte fell to the bottom of the well and remained at the lowest point. The microelectrode was scanned according to the z-direction from side point of sample (so-called "side-scanning": Fig. 1g, h). The motor driven XYZ-stage was located on the microscope stage for electrode tip scanning. The XYZ stage and potentiostat were controled by computer. The oxygen consumption rate of oocytes is calculated by newly designed software.

Oocyte collection and maturation culture

Pig cumulus-oocyte complexes (COCs) were obtained from ovarian follicles 2-5 mm in diameter. COCs classified as good quality by morphological evaluation were cultured in TCM199 medium containing 2.2 mg/ml sodium pyruvate, 10 mg/ml bovine serum albumin (BSA), 100 IU/ml penicillin, 100 μg/ml streptomycin, and 10% pig follicular fluid for *in vitro* maturation (IVM) in a humidified atmosphere of 5% CO_2 in air at 37.0°C for 48 h. After the cultures, cumulus cells were completely removed by the pipetting. The oxygen consumption of single denuded oocyte was measured by SECM systems. After the measurement, oocytes were prepared for histological (mitochondrial distribution) and biochemical (ATP content) experiments.

Staining of mitochondria

Oocytes were stained by MitoTracker Orange (Invitrogen;

Carlsbad, CA). This dye becomes fluorescent once it accumulates in the membrane lipids of mitochondria with membrane potential and is an important tool for evaluating the distribution of active mitochondria. MitoTracker Orange was used at a concentration of 350 nM in HPM199 medium (based on TCM199) supplemented 0.5% BSA for 30 min at 37.0°C. Oocytes were washed three times, mounted in a drop of HPM199 medium and examined using a confocal laser scanning microscope (FV-300; Olympus, Tokyo, Japan).

Measurement of the ATP content of oocytes

The ATP content of completely denuded oocyte was measured using a commercial assay based on the luciferin-luciferase reaction (Promega, Sunnyvale, Ca). Oocytes were rinsed three times in phosphate buffered saline (PBS), and then transferred individually in 50 uL of PBS into plastic tubes. Then, 50 uL of BacTiter-Glo reagent was added to all tubes were incubated for 5 min at room temperature. The ATP content of the samples was measured using a liminometer (Luminometer 20/20n, Promega) with high sensitivity (0.001 pmol). A five-point standard curve (0-10 pmole/tube) was routinely included in each assay. The ATP content was determined from the formula for the standard curve.

RESULTS AND DISCUSSION

Oxygen consumption of pig oocytes before and after *in vitro* maturation

Oxygen consumption rates of immature oocytes (immediately upon recovery from ovary) were 0.44×10^{14}/mol s^{-1}. In the maturation culture, a higher oxygen consumption rate was found in matured oocytes (with polar body extrusion), whereas the oxygen consumption rate of non-matured oocytes (without polar body extrusion) decreased during oocyte maturation (Table 1). These results showed that the oxygen consumption of pig oocytes changed in maturation status of oocytes.

Table 1. Oxygen consumption rates of pig oocytes in different maturaton status

Maturation status	O_2 consumption rate ($F\times 10^{14}$/mol · s^{-1})
Immature	0.44 ± 0.03^{a}
Mature	0.44 ± 0.03^{a}
Non-mature	0.21 ± 0.03^{b}

Values with different superscripts in each column are significantly different ($P < 0.05$).

Distribution of mitochondria in pig oocytes

Mitochondrial localization in oocytes after IVM is showed in Figure 2. The oocytes were classified in three types (Type-I, Type-II or Type-III) according to the pattern of active mitochondria distribution. Staining with MitoTracker orange revealed small mitochondrial clumps that were as a rule found in the periphery of the cytoplasm (Type-I). The Type-II oocytes showed the strong and homogeneous staining. In the oocytes classified as Type-III, mitochondrial clumps showing the strongest staining were seen in the central parts of the cytoplasm. The number of Type-II and Type-III oocytes gradually increased during the maturation culture. These results suggest that active mitochondria moved from the periphery to the central parts of the cytoplasm in oocytes during oocyte maturation. Similar mitochondrial reorganization has been reported in bovine oocytes before and after IVM [21].

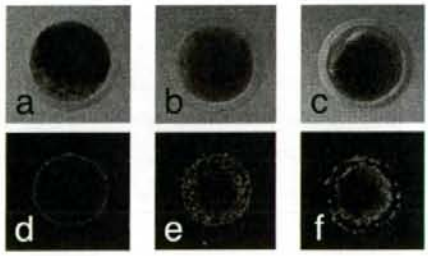

Fig. 2. Midline confocal sections of pig oocytes after maturation culture. a-c: Nomarski differential interference micrographs. d-f: Pig oocytes stained by MitoTracker orange. The oocytes are classified into three categories according to the mitochondria distribution, such as Type-I (a, d), Type-II (b, e), and Type-III (c, f).

Respiration rates and ATP content of different type of oocytes

The respiration rate and ATP content of Type-I oocyte were significantly lower than in Type-II and Type-III oocytes (Table 2). Although Type-II oocytes showed the high respiratory activity, they contained significantly less ATP than oocytes of Type-III oocytes. The average respiration rate and ATP content of Type-III

oocytes tended to be higher than that of other types of oocytes. These results demonstrated that the oxygen consumption rate and ATP content of pig oocytes was significantly affected by category of mitochondrial distribution. Type-II oocytes are thought to be an intermediate type between Type-I and Type-III oocyte in maturation status. This study suggests that there is a correlation between the respiratory activity and the maturation status of pig oocytes.

Table 2. Oxygen consumption rates of pig oocytes in different maturaton status

Category	O_2 consumption rate ($F \times 10^{14}$/mol · s^{-1})	ATP content (pmol/oocyte)
Type-I	0.20 ± 0.10^{a}	0.08 ± 0.01^{a}
Type-II	0.54 ± 0.02^{b}	1.66 ± 0.11^{b}
Type-III	0.53 ± 0.01^{b}	2.08 ± 0.05^{c}

Values with different superscripts in each column are significantly different ($P < 0.05$).

CONCLUSIONS

In this study, oxygen consumption by single pig oocytes was non-invasively and quantitatively determine by SECM measuring system. The biochemical and cytological studies strongly suggest that oxygen consumption is an important parameter to evaluate the competence of oocyte maturation in the pig. SECM measuring procedures can be used to accurately evaluate the metabolic activity and quality of pig oocytes.

ACKNOWLEDGEMENTS

This work was supported by Research and Development Program for New Bio-Industry Initiatives, Bio-oriented Technology Research Advancement Institution (BRAIN), Grant-in-Aid for Scientific Research (17380164), on Priority Areas "Lifesurveyor" (19021006) from the Ministry of Education, Culture, Sports, Science and Technology of Japan, Special Coordination Funds for Promoting Science and Technology of Japan, and the Japan Livestock Technology Association.

REFERENCES

[1] R.M. Mills and R.L. Brinster, *Exp. Cell Res.*, 47, 337-44 (1967).

[2] B. Nilsson, C. Magnusson, S. Widehn and T. Hillensjo, *J. Embryol. Exp. Morphol.*, 71, 75-82 (1982).

[3] C. Magnusson, T. Hillensjo, L. Hamberger and L. Nilsson, *Hum. Reprod.*, 1, 183-4 (1986).

[4] J.G. Thompson, R.J. Partridge, F.D. Houghton, C.I. Cox and H.J. Leese, *J. Reprod. Fertil.*, 106, 299-306 (1996).

[5] I. Donnay and H.J. Leese, *Mol. Reprod. Dev.*, 53, 171-8 (1999).

[6] J.R. Trimarchi, L. Liu, D.M. Porterfield, P.J.S. Smith and D.L. Keefe, *Biol. Reprod.*, 62, 1866-74 (2000).

[7] A.J. Bard and M.V. Mirkin,"Scanning Electrochemical Microscopy", Marcel Dekker Inc., New York (2000).

[8] K. Yamashita, M. Takagi, K. Uchida, H. Kondo and S. Takenaka, *Analyst*, 26, 1210-11 (2001).

[9] D. Oyamatsu, N. Kanaya,, H. Shiku, M. Nishizawa and T. Matsue, *Sens. Actuat. B: Chem.*, 91, 199-204 (2003).

[10] H. Shiku, T. Matsue and I. Uchida, *Anal. Chem.*, 68, 1276-8 (1996).

[11] S. Kasai, A.Z.H. Yokota, M. Nishizawa, K. Niwa, T. Onouchi and T. Matuse, *Anal. Chem.*, 72, 5761-5 (2001).

[12] H. Zhou, H. Shiku, S. Kasai, H. Noda, T. Matsue, H. Ohya-Nishiguchi and H. Kamada, *Bioelectrochemistry*, 54, 151-6 (2001).

[13] M. Nishizawa, K. Takoh and T. Matsue, *Langmuir*, 18, 3645-9 (2002).

[14] H. Shiku, T. Shiraishi, H. Ohya, T. Matsue, H. Abe, H. Hoshi and M. Kobayashi, *Anal. Chem.*, 73, 3751-8 (2001).

[15] H. Abe and H. Hoshi, *J. Reprod. Dev.*, 49, 193-202 (2003).

[16] H. Abe, H. Shiku, S. Aoyagi and H. Hoshi, *J. Mamm. Ova Res.*, 21, 22-30 (2004).

[17] L. Veek, *Ann. N.Y. Acad. Sci.*, 541, 259-74 (1988).

[18] H. Shiku, T. Shiraishi, S. Aoyagi, Y. Utsumi, M. Matsudaira, H. Abe, H. Hoshi, S. Kasai, H. Ohya and T. Matsue, *Anal. Biochim. Acta*, 522, 51-8 (2004).

[19] T. Matsue, S. Koike and I. Uchida, *Biochem. Biophys. Res. Commun.*, 197, 1283-7 (1993).

[20] P. Quinn, J.K. Kerin and G.M. Warnes, *Fertil. Steril.*, 44, 493-8 (1985).

[21] M. Stojkovic, S.A. Machado, P. Stojkovic, V. Zakhartchenko, P. Hutzler, P.B. Goncalves and E. Wolf, *Biol. Reprod.*, 64, 904-9 (2001).

(Recieved December 9, 2007 ; Accepted April 5, 2008)

ZOOLOGICAL SCIENCE 25: 1057–1065 (2008)

Mitochondria are More Numerous and Smaller in Pink-Eyed Dilution Melanoblasts and Melanocytes Than in Wild-Type Melanocytes in the Neonatal Mouse Epidermis

Tomohisa Hirobe[1,2*], Kenji Ishizuka[3], Shigeru Ogawa[3] and Hiroyuki Abe[4]

[1]*Radiation Effect Mechanism Research Group, National Institute of Radiological Sciences, Chiba 263-8555, Japan*
[2]*Graduate School of Science, Chiba University, Chiba 263-8522, Japan*
[3]*Graduate School of Education, Joetsu University of Education, Joetsu 943-8512, Japan*
[4]*Graduate School of Science and Engineering, Yamagata University, Yonezawa 992-8510, Japan*

The mouse pink-eyed dilution (*p*) locus is known to control the melanin content in melanocytes. However, it was not known whether the *p* gene is involved in regulating the proliferation and differentation of melanocytes during development, especially the biogenesis of melanosomes and other organelles. Epidermal cell suspensions of neonatal dorsal skin derived from mice wild type for the *p* locus (black, C57BL/10JHir-*P/P*) and their congenic mutant phenotype (pink-eyed dilution, C57BL/10JHir-*p/p*) were cultured in serum-free melanocyte-proliferation medium (MDMD). The supplement of additional L-tyrosine (Tyr) into the MDMD stimulated the differentiation of *p/p* melanoblasts into melanocytes. Electron microscopy revealed that in *p/p* melanoblasts and melanocytes treated with L-Tyr, the number of stage II and III melanosomes dramatically increased. Moreover, *p/p* melanoblasts possessed smaller but more numerous mitochondria than *P/P* melanocytes. The treatment of *p/p* melanoblasts and melanocytes with L-Tyr decreased the number of mitochondria. The supplement of 2, 4-dinitrophenol (DNP), an inhibitor of mitochondrial function, into the MDMD stimulated both the proliferation and differentiation of *p/p* melanoblasts. Simultaneous treatment of DNP and L-Tyr dramatically stimulated the differetiation of *p/p* melanocytes. These results suggest that L-Tyr and some unknown factors related to mitochondrial function may influence the differentiation of melanoblasts in the epidermis of *p/p* mice.

Key words: pink-eyed dilution, melanocyte, melanoblast, mitochondria

INTRODUCTION

Mouse epidermal melanocytes differentiate around the time of birth (Hirobe, 1984) from undifferentiated precursors, melanoblasts, which originate from the neural crest in the embryo (Rawles, 1947; Mayer, 1973). They increase in number until 3 or 4 days after birth, and then their numbers decrease (Hirobe, 1984). Most epidermal melanocytes migrate into hair bulbs, and pigment-accumulating organelles, melanosomes (Seiji et al., 1963), are transported to surrounding keratinocytes to produce pigmented hairs. Differentiated melanocytes produce two types of melanin: brownish-black eumelanin and reddish-yellow pheomelanin (Prota, 1980; Ito, 2003).

Numerous coat-color genes are involved in regulating the development of murine melanocytes (Silvers, 1979). The mouse pink-eyed dilution (*p*) locus controls the melanin content in melanocytes and in the retinal pigment epithelium (Silvers, 1979). In mouse hairs, the *p* mutation drastically reduces the eumelanin content (Silvers, 1979). In addition to a reduction in the amount of eumelanin deposited (Ozeki et al., 1995), melanin granules within the hair shafts of *p/p* mice are smaller than those in *P/P* mice (Russell, 1949). The *p/p* melanocytes contain smaller and rounder (Markert and Silvers, 1956, Orlow and Brilliant, 1999), immature (Sidman and Pearlstein, 1965; Moyer, 1966; Hearing et al., 1973; Hirobe and Abe, 1999) melanosomes, and the numbers of stage III and IV melanosomes are much fewer than in *P/P* melanocytes (Hirobe et al., 2002b).

Levels of tyrosinase, the rate-limiting enzyme in melanin synthesis, are greatly decreased in the skin of *p/p* mice (Tamate et al., 1989) and in cultured epidermal melanocytes of newborn *p/p* mice (Hirobe et al., 1998). The product of the *p* gene is an integral membrane protein that localizes in melanosomes (Rosemblat et al., 1994); its predicted secondary structure is a 12-transmembrane domain protein similar to a channel or transporter (Gardner et al., 1992; Rinchik et al., 1993). Excess tyrosine (Tyr) in a culture medium can greatly stimulate the pigmentation of retinal pigment epithelial cells and choroidal melanocytes from *p/p*

* Corresponding author. Phone: +81-43-206-3253/3133;
Fax : +81-43-206-4638;
E-mail: thirobe@nirs.go.jp
doi:10.2108/zsj.25.1057

mice (Sidman and Peatstein, 1965), suggesting that *p* protein functions as a Tyr transporter. Other groups suggest that the *p* protein is involved in regulating the maturation of melanosomes and the stabilization or trafficking of melanosomal membrane proteins (Lamoreux et al., 1995; Rosemblat et al., 1998; Orlow and Brilliant, 1999). Another theory that the *p* protein is a transporter that controls melanosomal acidification (Puri et al., 2000; Brilliant, 2001) has also been presented. The *p* protein also controls the processing and transport of tyrosinase (Chen et al., 2002; Toyofuku et al., 2002). Moreover, the *p* protein is reported to increase cellular sensitivity to arsenicals and other metalloids and to modulate intracellular glutathione metabolism (Staleva et al., 2002). It has also been proposed that the *p* protein mediates neutralization of melanosomal pH (Ancas et al., 2001). In addition, the proliferation and differentiation of neonatal mouse melanocytes are greatly inhibited by the *p* mutation (Hirobe and Abe, 1999; Hirobe et al., 2002a, b), and excess L-Tyr supplemented to the culture medium rescues both proliferative and differentiative activities of *p/p* melanoblasts (Hirobe et al., 2002b). Furthermore, the differentiation of melanoblasts into melanocytes is gradually induced by L-Tyr as the age of the donor mice advances, even though eumelanin and pheomelanin fail to accumulate in *p/p* melanocytes and are released from them at all stages of skin development (Hirobe et al., 2003a). This observation was confirmed by a study that showed that in 7.5-day-old *p/p* mice, the plasma levels of a eumelanin-related metabolite, 6-hydroxy-5-methoxyindole-2-carboxylic acid, and a pheomelanin-related metabolite, 5-*S*-cysteinyldopa, were nine-fold and four-fold greater, respectively, than in 7.5-day-old *P/P* mice (Wakamatsu et al., 2007).

However, it was not known whether the *p* mutation affects the biogenesis of melanosomes and other organelles in melanocytes in serum-free primary culture. In this study, we observed in detail, by using electron microscopy, the biogenesis of melanosomes and other organelles in cultured *p/p* melanoblasts with or without L-Tyr.

MATERIALS AND METHODS

Mice

All animals used in this study belonged to the strain C57BL/10JHir (B10, black, *P/P*) and its congenic strain, B10-*p/p* (pink-eyed dilution, *p/p*) of the house mouse, *Mus musculus*. They were given water and a commercial diet, OA-2 (Clea Japan, Tokyo, Japan) ad libitum. Congenic B10-*p/p* mice were established in our laboratory (Hirobe, 1986). Originally, the mutation (*p*) was introduced into B10 animals with nine generations of continued backcrossing followed by sib mating (Hirobe, 1986). After the 20th generation of sib mating, the congenic mice were continuously backcrossed with B10 for at least three generations, followed by sib mating. This procedure was then repeated. The genic constitution of the line differs only in the *p* locus. They were maintained at 24±1°C with 40–60% relative humidity; 12 hr of fluorescent light were provided daily. This study was approved by the ethics committee of the National Institute of Radiological Sciences in accordance with the guidelines of the National Institute of Health.

Melanocyte primary culture

The source of tissue for the culture of melanoblasts and melanocytes was dorsal skin from 0.5-day-old *P/P* and *p/p* mice. Unless stated otherwise, all reagents were purchased from Sigma Chemical Co. (St. Louis, MO, USA). The method for obtaining epidermal cell suspensions was reported previously (Hirobe et al., 2002a, b). Disaggregated epidermal cell suspensions were pelleted by centrifugation and suspended in Ham's F-10 medium (Gibco, Grand Island, NY, USA). The cell pellet after centrifugation was resuspended in melanocyte-proliferation medium (MDMD) consisting of Ham's F-10 plus 10 μg/ml bovine insulin, 0.5 mg/ml bovine serum albumin (Fraction V), 1 μM ethanolamine, 1 μM phosphoethanolamine, 10 nM sodium selenite, 0.5 mM dibutyryl adenosine 3':5'-cyclic monophosphate (DBcAMP), 100 U/ml penicillin G, 100 μg/ml streptomycin sulfate, 50 μg/ml gentamycin sulfate, and 0.25 μg/ml amphotericin B. The same lots of these supplements were used in this study. Cells in each epidermal cell suspension were counted in a hemocytometer and were plated onto dishes coated with type-I collagen (Becton Dickinson, Bedford, MA, USA) an initial density of 1×10^6 cells/35 mm dish (1.04×10^5 cells/cm^2). Cultures were incubated at 37°C in a humidified atmosphere of 5% CO_2 and 95% air (pH 7.2). The medium was replaced with fresh medium four times a week. After 14 days, pure cultures of melanoblasts (*p/p*) or melanocytes (*P/P*) were obtained. In some cases, additional L-Tyr (2 mM) was added to the medium from initiation of the primary culture. The standard concentration of L-Tyr in Ham's F-10 is 10 μM. Moreover, 2, 4-dinitrophenol (DNP) was added to the medium at concentrations of 0.01, 0.1, and 1 μM from initiation of the primary culture.

Assays for proliferation and differentiation

The number of melanoblasts and melanocytes was determined per dish by phase-contrast and bright-field microscopy; the calculation was based on the average number of cells from 10 randomly chosen microscopic fields covering an area of 0.581 mm^2. Bipolar, tripolar, dendritic, polygonal, or epithelioid cells, as seen in phase-contrast, that contained brown or black pigment granules, as observed by bright-field microscopy, were scored as pigmented melanocytes. In contrast, bipolar, tripolar, dendritic, or polygonal cells, as seen in phase-contrast, that contained no pigments and were negative (no tyrosinase activity) to 3, 4-dihydroxyphenylalanine (dopa) were scored as melanoblasts. These cells were stained by the combined dopa-premelanin reaction (combined dopa-ammoniacal silver nitrate staining; Mishima, 1960; Hirobe, 1984). This preferential staining reveals undifferentiated melanoblasts that contain stage I and II melanosomes without tyrosinase activity, in addition to tyrosinase-containing differentiated melanocytes. The ammoniacal silver nitrate reaction specifically reveals both unmelanized melanosomes and melanized melanosomes in melanocytes, the metallic silver particles being deposited with a high degree of selectivity (Mishima, 1960; Hirobe, 1984). Melanoblasts were also stained by antibodies to the tyrosinase-related proteins TRP-1 and TRP-2 (Hirobe et al., 2002a). A "melanoblast" is defined here as an unpigmented cell that possesses no tyrosinase activity. The statistical significance of differences was determined by Student's *t*-test for comparisons of groups of equal size.

Electron microscopy

Pure primary *P/P* and *p/p* melanoblasts/melanocytes cultured for 3, 7, and 14 days were treated with a solution of 0.05% trypsin (Difco, Sparks, MD, USA) and 0.02% ethylenediaminetetraacetate in Ca^{2+}-, Mg^{2+}-free phosphate buffered saline at 37°C for 10 min. After trypsinization was inhibited by addition of 2000 U/ml of soybean trypsin inhibitor, the cell suspensions were centrifuged at 1500 rpm for 5 min. The cell pellets were fixed in chilled (2°C) 2.5% glutaraldehyde (Taab Laboratories Equipment Ltd., Berkshire, UK) in 0.1 M phosphate buffer (pH 7.4). After washing with chilled 0.1 M phosphate buffer, the cells were postfixed in chilled 1% osmium tetroxide (Taab Laboratories Equipment Ltd.) in 0.1 M phosphate buffer. After washing again with chilled 0.1 M phosphate buffer, the

cells were dehydrated in a graded ethanol series and embedded in epoxy resin (Taab Laboratories Equipment Ltd.). Ultrathin sections were cut with a diamond knife on an ultramicrotome (Leica, Heerbrugg, Switzerland), stained with uranyl acetate and lead citrate, and examined with a transmission electron microscope (JEM-2000 EX, JEM, Tokyo, Japan).

One hundred electron micrographs of cells in each group were surveyed for the presence of stage I, II, III, and IV melanosomes, Golgi apparatus, mitochondria, and lysosomes, which were scored, and the numbers of these organelles per unit area (100 μm^2) were calculated. The size of mitochondria was estimated as the area of an ellipse (πab), calculated after measurement of the major (a) and minor (b) axes. The total number of mitochondria measured was 100 for each group.

Melanosome development was categorized in the four stages defined by Fitzpatrick et al. (1969): Stage I melanosomes initiate the accumulation of intralumenal fibrils; stage II melanosomes possess completed intralumenal fibrils without pigment; stage III melanosomes possess longitudinal depositions of pigment in intralumenal fibrils; stage IV melanosomes are fully deposited with pigment.

RESULTS

Light-microscopic observations

Within 1 day after the initiation of epidermal cell suspensions derived from 0.5-day-old *P/P* mice in MDMD, small keratinocyte colonies could be seen. Small bipolar or tripolar cells (melanoblasts) were scattered between the keratino-

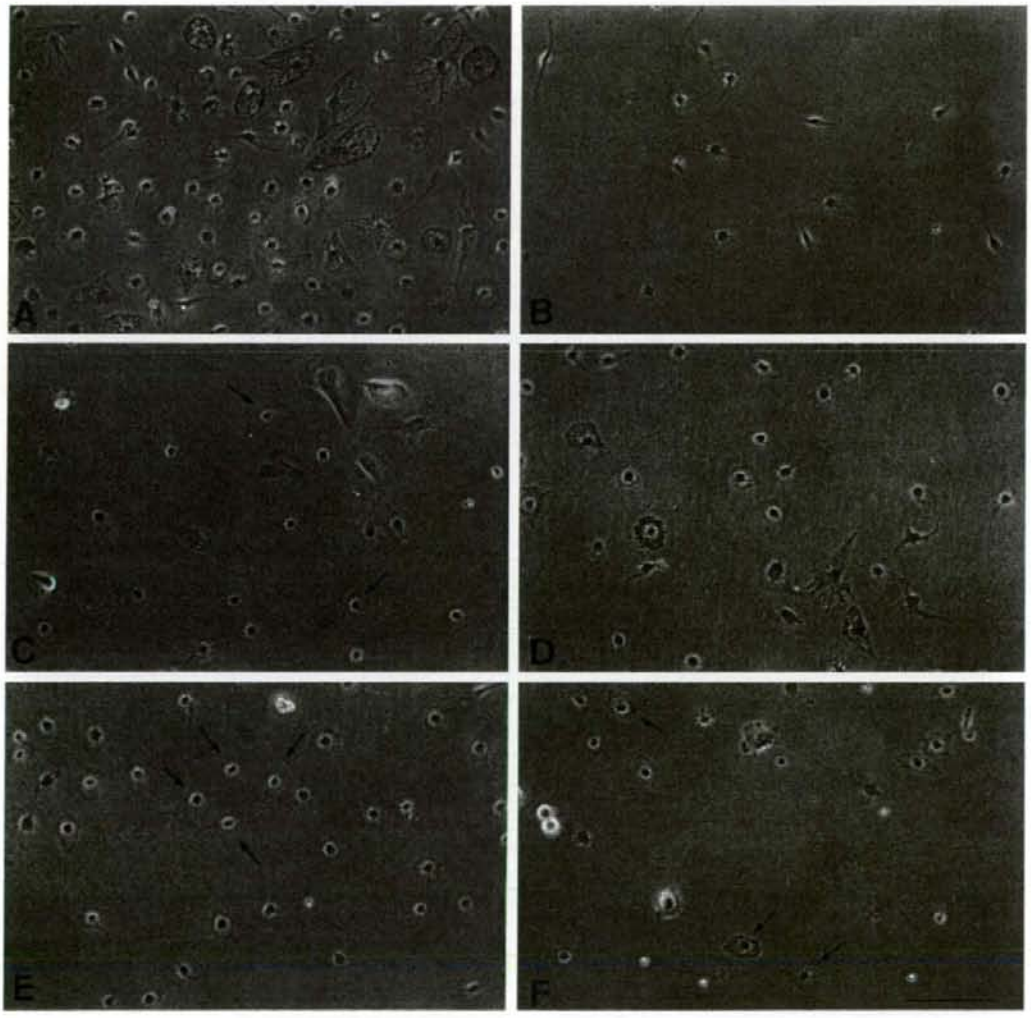

Fig. 1. Melanoblasts and melanocytes derived from epidermal cell suspensions of 0.5-day-old *P/P* **(A, D)** and *p/p* **(B, C, E, F)** mice. They were cultured with **(C)** or without **(A, B)** 2 mM L-Tyr. They were also cultured with 1 μM DNP **(D, E)** or with 1 μM DNP + 2 mM L-Tyr **(F)**. L-Tyr stimulated the differentiation of *p/p* melanoblasts into melanocytes after 14 days in culture. **(C)**; arrows indicate differentiated *p/p* melanocytes. DNP **(E)** as well as DNP + L-Tyr **(F)** stimulated the differentiation of *p/p* melanocytes. Arrows indicate differentiated melanocytes **(E, F)**. Phase-contrast microscopy. Scale bar, 100 μm.

cyte colonies. After 2 or 3 days, pigment granules appeared in the cytoplasm and processes of melanoblasts. After 4 or 5 days, melanocytes increased in number. They were more pigmented than before and extended dendrites into the surrounding keratinocytes. After 8 or 9 days, the keratinocyte colonies gradually decreased in number, and by 12–14 days, cultures contained pure melanocytes with intense pigmentation (Fig. 1A). When epidermal cell suspensions from *p/p* mice were cultured in MDMD, a similar proliferation of keratinocytes was observed. However, the proliferation and differentiation of melanoblasts were greatly inhibited. No pigmented melanocytes were found during the culture (Fig. 1B). When epidermal cell suspensions from *p/p* mice were cultured with L-Tyr (2 mM), keratinocyte proliferation showed no change. However, many differentiated melanocytes appeared; the percentage of melanocytes in the melanoblast-melanocyte population gradually increased (Fig. 1C), and exceeded 40% at 14 days.

Electron-microscopic observations

Electron microscopic observations showed that melanosomes of *P/P* melanocytes cultured for 14 days (Fig. 2A) were ellipsoidal or ovoid, with intralumenal depositions of melanin. Mature stage IV melanosomes were predominant in *P/P* melanocytes (Fig. 2A). Golgi apparatus and mitochondria were also observed (Fig. 2A). On the other hand, *p/p* melanoblasts cultured for 14 days possessed a few stage I and II melanosomes, whereas they possessed numerous Golgi apparatus and mitochondria (Fig. 2B). No stage III and IV melanosomes were found (Fig. 2B). However, excess L-Tyr dramatically increased stage II and III melanosomes in *p/p* cells cultured for 14 days (Fig. 2C). This increase in the number of stage II and III melanosomes was much higher than that in stage IV melanosomes (Fig. 2C).

The number of Golgi apparatus in *p/p* melanoblasts was much greater than in *P/P* melanocytes (Fig. 3A). The number (*p/p*) increased as culture proceeded (Fig. 3A). The number of Golgi apparatus in *p/p* melanoblasts at 14 days was four-fold greater than in *P/P* melanocytes (Fig. 3A). L-Tyr decreased the number of Golgi apparatus in *p/p* melanoblasts/melanocytes, though the number was still higher than in *P/P* melanocytes (Fig. 3A). Although why the number of Golgi apparatus in *p/p* cells cultured with L-Tyr at 3 days is high cannot be explained well at present, L-Tyr possibly stimulates the development of Golgi apparatus to induce the differentiation (de novo stage III and IV melanosome formation) of *p/p* melanocytes. The number of Golgi apparatus may gradually decrease with increasing formation of melanosomes during culture.

The numbers of mitochondria in *p/p* melanoblasts at 3, 7, and 14 days were roughly two-, four-, and five-fold greater than in *P/P* melanocytes, respectively (Fig. 3B). L-Tyr decreased the number of mitochondria in *p/p* melanoblasts/melanocytes, though the number was still higher than in *P/P* melanocytes (Fig. 3B). The size of mitochondria in *p/p* melanoblasts was smaller than in *P/P* melanocytes (Fig. 4), suggesting that mitochondria in *p/p* melanoblasts may divide, and this division may produce more numerous and smaller mitochondria. L-Tyr failed to increase the size of mitochondria in *p/p* melanoblasts/melanocytes.

Fig. 2. Electron micrographs of epidermal *P/P* melanocytes **(A)** and *p/p* melanoblasts **(B)** or melanocytes **(C)** cultured for 14 days in MDMD with **(C)** or without **(A, B)** 2 mM L-Tyr. **(A)** Numerous stage III and IV melanosomes (indicated in the figure by corresponding roman numberals) are seen in *P/P* melanocytes. **(B)** In contrast, only a small number of stage I and II melanosomes are seen in *p/p* melanoblasts. In *p/p* melanoblasts **(B)**, well-developed Golgi apparatus (G) and mitochondria (M) are seen. However, in *p/p* melanocytes cultured with 2 mM L-Tyr **(C)**, all stages (I, II, III, and IV) of melanosomes are seen, including numerous stage III melanosomes. Scale bar, 1 μm.

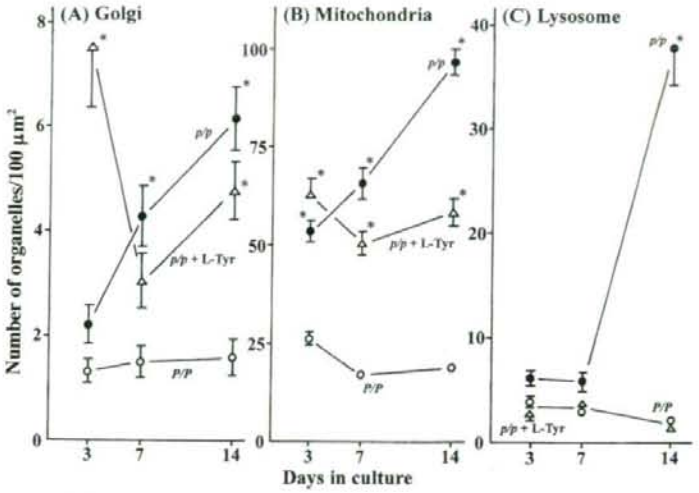

Fig. 3. Changes in the number of **(A)** Golgi apparatus, **(B)** mitochondria, and **(C)** lysosomes in cultured *P/P* melanocytes, *p/p* melanoblasts, and *p/p* melanoblasts/melanocytes in the presence of 2 mM L-Tyr. Epidermal cell suspensions were derived from 0.5-day-old mice and cultured for 14 days. The cells were fixed at 3, 7, and 14 days, and 100 melanoblasts or melanocytes for each group were recorded for the detection of organelles. The number of Golgi apparatus **(A)** in *p/p* melanoblasts is more numerous than in *P/P* melanocytes. The number of Golgi apparatus in *p/p* melanoblasts increased dramatically as the culture proceeded. L-Tyr reduced the number of Golgi apparatus, though the number still exceeded that of *P/P* melanocytes. The number of mitochondria **(B)** in *p/p* melanoblasts is much greater than in *P/P* melanocytes. The number of mitochondria in *p/p* melanoblasts increased dramatically as the culture proceeded. L-Tyr decreased the number of mitochondria, though the number was still higher than in *P/P* melanocytes. The number of lysosomes **(C)** in *p/p* melanoblasts is higher than in *P/P* melanocytes, especially at 14 days. L-Tyr completely reduced the number of lysosomes in *p/p* melanoblasts/melanocytes, which was comparable to that in *P/P* melanocytes. The data are the averages of results from 100 electron micrographs of cells. Bars indicate the standard error of the mean (SEM) and are shown only when they were larger than the symbols. **P*<0.05.

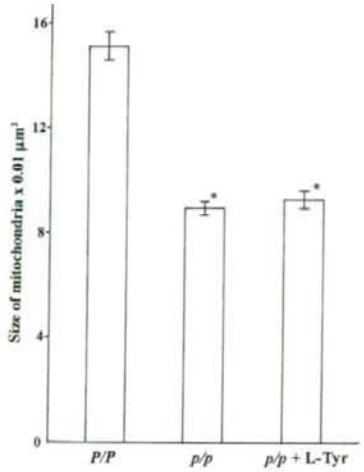

Fig. 4. Size of mitochondria in *P/P* melanocytes, *p/p* melanoblasts, and *p/p* melanoblasts/melanocytes cultured with 2 mM L-Tyr. Epidermal cell suspensions were derived from 0.5-day-old mice and cultured for 7 days. The cells were fixed, and size measurements were made for 100 mitochondria. The size of mitochondria in *p/p* melanoblasts is smaller than in *P/P* melanocytes. L-Tyr failed to increase the size of mitochondria in *p/p* melanoblasts/melanocytes. The data are the averages of results from 100 mitochondria in electron micrographs of cells. Bars indicate SEM. **P*<0.05.

The number of lysosomes in *p/p* melanoblasts was greater than in *P/P* melanocytes, especially at 14 days (Fig. 3C). L-Tyr completely reduced the number of lysosomes in *p/p* melanoblasts/melanocytes, and the number was comparable to that in *P/P* melanocytes (Fig. 3C).

These results suggest the possibility that changes in Golgi apparatus, mitochondria, and lysosomes in *p/p* melanoblasts may influence the formation and maturation of melanosomes.

Effects of DNP on melanocytes

In *P/P* melanocytes, the proliferation of melanocytes was inhibited by DNP, an inhibitor of mitochondrial function (Figs. 1D, 5A), though the differentiation of melanocytes was not affected (Figs. 1D, 5D). In contrast, in *p/p* melanoblasts, both proliferation (Figs. 1E, 5B) and differentiation (Figs. 1E, 5E) were stimulated by DNP. The number of melanoblasts and melanocytes was significantly increased at 14 days by DNP treatment at a concentration of 1 μM (Fig. 5B, $P<0.05$), and many mitotic figures of *p/p* melanoblasts and melanocytes cultured with DNP were observed. Moreover, the percentage of melanocytes in the melanoblast-melanocyte population was also increased at 7 and 14 days at all concentrations tested (0.01, 0.1, 1 μM; $P<0.05$). Ca. 20% of cells were induced to differentiate at 1 μM DNP at 14 days (Fig. 5E). Simultaneous treatment with DNP and L-Tyr resulted in a greater increase in the percentage of melanocytes in the melanoblast-melanocyte population (Figs. 1F,

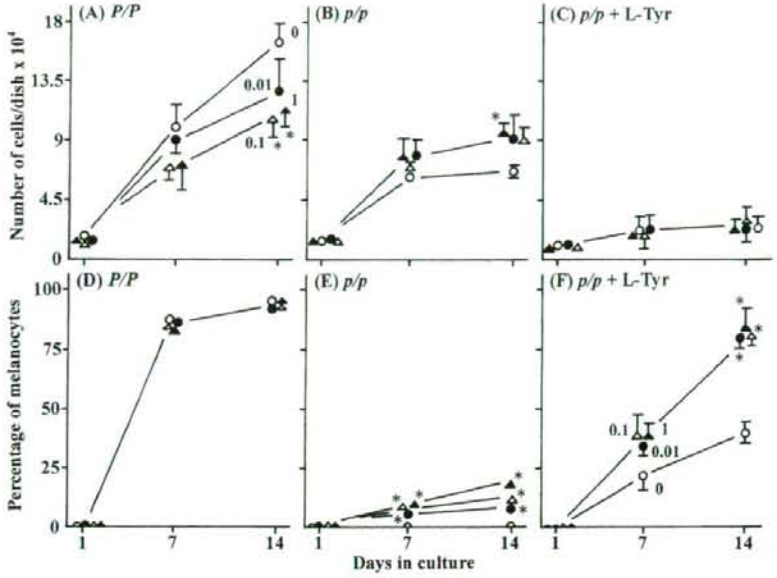

Fig. 5. Kinetics of the proliferation **(A, B, C)** and differentiation **(D, E, F)** of epidermal *P/P* melanocytes **(A, D)**, *p/p* melanoblasts **(B, E)**, and *p/p* melanoblasts/melanocytes cultured with 2 mM L-Tyr **(C, F)**. Epidermal cell suspensions were derived from 0.5-day-old mice. DNP at concentrations of 0 (○), 0.01 (●), 0.1 (△), and 1 (▲) μM was added to each culture from initiation of the primary culture. Pure cultures of melanoblasts or melanocytes were obtained after 14 days. The number of melanoblasts and melanocytes was counted by phase-contrast and bright-field microscopy at 1, 7, and 14 days. The data are the averages of results from three experiments. Each experiment was performed with different litters of mice. Bars indicate the SEM and are shown only when they were larger than the symbols. *$P<0.05$.

5F). More than 80% of cells were differentiated at 14 days at all concentrations tested (Fig. 5F; $P<0.05$). However, the proliferation of melanoblasts and melanocytes was not stimulated by simultaneous treatment with DNP and L-Tyr (Fig. 5C). These results suggest that DNP may rescue the reduced proliferation and differentiation of *p/p* melanoblasts, and that DNP may restore the reduced differentiation of *p/p* melanoblasts in cooperation with L-Tyr.

DISCUSSION

Our present study demonstrated that the proliferative and differentiative activity of *p/p* melanoblasts cultured from neonatal murine epidermis was greatly reduced compared with that of *P/P* melanocytes. The differentiative activity of *p/p* melanoblasts in culture was increased by the addition of L-Tyr to MDMD in this study. Our previous study showed that L-Tyr increased the tyrosinase activity of *p/p* melanocytes in primary culture (Hirobe et al., 2002b). It is possible that increased tyrosinase activity in cultured *p/p* melanocytes by L-Tyr stimulates their differentiation. The question arises as to what mechanisms are involved in regulation by L-Tyr of the differentiation of *p/p* melanocytes. One possible explanation is that L-Tyr acts directly on melanocytes and activates factors involved in regulating signal transduction pathways required for cell differentiation, such as the protein kinase A (PKA; Hirobe, 1992), tyrosine kinase (TK, Coughlin et al., 1988), and PKC (Imokawa et al., 1997) pathways. Indeed, in mouse melanoma cells, L-Tyr stimulates the capacity of melanocyte-stimulating hormone (MSH) to bind the MSH receptor, and consequently the PKA pathway is activated through the elevation of cAMP level in the cells (Slominski et al., 1989). Thus, the activation of PKA is thought to stimulate the differentiation of *p/p* melanocytes. Another explanation is that L-Tyr acts on the tissue environment, especially keratinocytes, and induces or stimulates the synthesis of melanogens, such as MSH (Thody et al., 1983), basic fibroblast growth factor (Halaban et al., 1988), nerve growth factor (Yaar et al., 1991), endothelins (Yada et al., 1991; Imokawa et al., 1992; Yohn et al., 1993; Hirobe, 2001), granulocyte macrophage colony-stimulating factor (Imokawa et al., 1996; Hirobe et al., 2004a), steel factor (Kunisada et al., 1998; Hirobe et al., 2003b), hepatocyte growth factor (Kunisada et al., 2000; Hirobe et al., 2004b), and leukemia inhibitory factor (Hirobe, 2002). This hypothesis may be partially supported by the observation that L-Tyr failed to stimulate the differentiation of cultured melanocytes in the absence of keratinocytes (Hirobe et al., 2002b).

Our present study showed that the formation and maturation of melanosomes was greatly inhibited in *p/p* melanoblasts, but that L-Tyr induced the de-novo formation and maturation of melanosomes. Although L-Tyr dramatically increased stage II and III melanosomes, mature stage IV melanosomes were not dramatically increased. These results suggest that the rescue by L-Tyr of the impaired melanocyte differentiation is incomplete, and that other, additional factors are required for the complete rescue.

Our present study demonstrated that *p/p* melanoblasts possess much more Golgi apparatus than *P/P* melanocytes.

The number of Golgi apparatus in *P/P* melanocytes in the epidermis of newborn mice is known to decrease as the developmental age advances (Hirobe and Takeuchi, 1978). Since melanosomes may at least in part originate from Golgi apparatus (Seiji et al., 1963; Novikoff et al., 1968; Maul, 1969; Imokawa and Mishima, 1981; Hirobe, 1982), the latter is thought to gradually decrease in number with increasing formation of melanosomes. However, in this study, L-Tyr failed to reduce the number of Golgi apparatus in *p/p* melanoblasts/melanocytes. Although this discrepancy between *P/P* melanocytes and *p/p* melanoblasts/melanocytes cannot be fully explained at present, it might be attributed to differences in the formation and maturation of melanosomes between *P/P* melanocytes and *p/p* melanoblasts/melanocytes. In *P/P* melanocytes, the formation and maturation of melanosomes may be fully activated, and thus a small number of Golgi apparatus may exist under normal circumstances. In contrast, in *p/p* melanoblasts, the formation and maturation of melanosomes may not be fully activated, and thus a large number of Golgi apparatus may be present under normal circumstances. Moreover, the stimulation of melanosome formation and maturation by L-Tyr in *p/p* melanoblasts/melanocytes was incomplete (stage IV melanosomes did not increase greatly), and thus the number of Golgi apparatus failed to reach the level of *P/P* melanocytes. This hypothesis may be partially supported by the finding that the total numbers of both melanosomes and Golgi apparatus were not affected by the treatment with L-Tyr in cultured *P/P* melanocytes (Hirobe et al., 2007). Therefore, it is reasonable to assume that the number of Golgi apparatus in *p/p* melanoblasts is greater than in *P/P* melanocytes because of the reduced formation and maturation of melanosomes.

In our present study, *p/p* melanoblasts possessed many more lysosomes than *P/P* melanocytes, especially at 14 days in culture. In contrast, L-Tyr dramatically decreased the number of lysosomes at all days tested, and their numbers were comparable to those of *P/P* melanocytes. These results suggest that the increased melanosome formation and maturation induced by L-Tyr in *p/p* melanoblasts/melanocytes may elicit the decrease in the number of lysosomes. Melanosomes are thought to be specialized organelles of lysosomes (Orlow, 1995). Indeed in the *P/P* mouse epidermis, differentiated melanocytes possess a small number of lysosomes, whereas undifferentiated melanoblasts possess many lysosomes (Hirobe and Takeuchi, 1978). The relationship between melanosome formation and lysosome formation should be precisely investigated in a future study.

In our present study, many more mitochondria were present in *p/p* melanoblasts than in *P/P* melanocytes. Moreover, the number of mitochondria increased as the culture proceeded. L-Tyr decreased the number of mitochondria in *p/p* melanoblasts and melanocytes, though the number was still greater than in *P/P* melanocytes. From these results, we assume that the mitochondria in *p/p* melanoblasts influence the formation and maturation of melanosomes. This assumption may be partially supported by the findings that L-Tyr decreased the number of mitochondria in *p/p* melanoblasts/melanocytes, whereas L-Tyr increased the number of melanosomes. The size of mitochondria in *p/p* melanoblasts was smaller than in *P/P* melanocytes. Therefore, it is reasonable to conclude that the division of mitochondria may occur in *p/p* melanoblasts, resulting in numerous small-sized mitochondria. Although the theory that melanosomes originate from mitochondria (du Buy et al., 1963) was not supported by the study of Seiji et al. (1963), in the present study we propose the new theory that mitochondria may influence the formation and maturation of melanosomes in melanocytes by an unknown mechanism.

DNP inhibits oxidative phosphorylation in mitochondria (Han et al., 2008). In our present study, this inhibition of mitochondrial function by DNP stimulated the proliferation and differentiation of *p/p* melanoblasts. In contrast, DNP inhibited the proliferation of *P/P* melanocytes, whereas it did not affect the differentiation of *P/P* melanocytes. Therefore, it is reasonable to conclude that the dysfunction of mitochondria caused by DNP in *P/P* melanocytes may inhibit cell proliferation, due to a reduced energy supply. In contrast, the dysfunction of mitochondria caused by DNP in *p/p* melanoblasts may stimulate the proliferation of melanocytes, without a severe reduction in the energy supply, since *p/p* melanoblasts possess numerous mitochondria. DNP possibly stimulates the signaling pathway of PKA, PKC, and TK, and consequently the proliferation and differentiation of *p/p* melanoblasts are increased. This hypothesis may be partially supported by our findings that DNP and L-Tyr synergistically stimulated the differentiation of *p/p* melanoblasts.

Taken together, our present results suggest that the *p* gene exerts its influence by affecting the proliferation and differentiation of melanocytes through regulating melanosome formation and maturation, or through regulating the uptake of L-Tyr and the function of other organelles.

ACKNOWLEDGMENTS

This work was supported in part by Grants-in-Aid for Scientific Research (Nos. 14570829, 16591122, and 18591262) from the Japan Society for the Promotion of Science.

REFERENCES

Ancas A, Tobin DJ, Hoogduijn MJ, Smit NP, Wakamatsu K, Thody AJ (2001) Melanosomal pH controls rate of melanogenesis, eumelanin/pheomelanin ratio and melanosomal maturation in melanocytes and melanoma cells. Exp Cell Res 268: 26–35

Brilliant MH (2001) The mouse *p* (pink-eyed dilution) and human *P* genes, oculocutaneous albinism type 2 (OCA2), and melanosomal pH. Pigment Cell Res 14: 86–93

Chen K, Manga P, Orlow SJ (2002) Pink-eyed dilution protein controls the processing of tyrosinase. Mol Biol Cell 13: 1953–1964

Coughlin SR, Barr PJ, Cousens LS, Fretto LJ, Williams LT (1988) Acidic and basic fibroblast growth factors stimulate tyrosine kinase activity *in vivo*. J Biol Chem 263: 988–993

du Buy HG, Showacre JL, Hesselbach ML (1963) Enzymic and other similarities of melanoma granules and mitochondria. Ann NY Acad Sci 100: 569–583

Fitzpatrick TB, Hori Y, Toda K, Seiji M (1969) Melanin 1969: some definitions and problems. Jpn J Dermatol B 79: 278–282

Gardner JM, Nakatsu Y, Gondo Y, Lee S, Lyon MF, King RA, Brilliant MH (1992) The mouse pink-eyed dilution gene: association with human Prader-Willi and Angelman syndromes. Science 257: 1121–1124

Han YH, Kim SW, Kim SH, Kim SZ, Park WH (2008) 2,4-dinitrophenol induces G1 phase arrest and apoptosis in human pulmonary

adenocarcinoma Calu-6 cells. Toxicol In Vitro 22: 659–670
Halaban R, Langdon R, Birchall N, Cuono C, Baird A, Scott G, Moellmann G, McGuire J (1988) Basic fibroblast growth factor from human keratinocytes is a natural mitogen for melanocytes. J Cell Biol 107: 1611–1619
Hearing VJ, Phillips P, Lutzner MA (1973) The fine structure of melanogenesis in coat color mutants of the mouse. J Ultrastruct Res 43: 88–106
Hirobe T (1982) Origin of melanosome structures and cytochemical localizations of tyrosinase activity in differentiating epidermal melanocytes of newborn mouse skin. J Exp Zool 224: 355–363
Hirobe T (1984) Histochemical survey of the distribution of the epidermal melanoblasts and melanocytes in the mouse during fetal and postnatal periods. Anat Rec 208: 589–594
Hirobe T (1986) Congenic strains of C57BL/10JHir. Mouse News Lett 76: 28–29
Hirobe T (1992) Control of melanocyte proliferation and differentiation in the mouse epidermis. Pigment Cell Res 5: 1–11
Hirobe T (2001) Endothelins are involved in regulating the proliferation and differentiation of mouse epidermal melanocytes in serum-free primary culture. J Invest Dermatol Symp Proc 6: 25–31
Hirobe T (2002) Role of leukemia inhibitory factor in the regulation of the proliferation and differentiation of neonatal mouse epidermal melanocytes in culture. J Cell Physiol 192: 315–326
Hirobe T, Abe H (1999) Genetic and epigenetic control of the proliferation and differentiation of mouse epidermal melanocytes in culture. Pigment Cell Res 12: 147–163
Hirobe T, Takeuchi T (1978) Changes of organelles associated with the differentiation of epidermal melanocytes in the mouse. J Embryol Exp Morph 43: 107–121
Hirobe T, Wakamatsu K, Ito S (1998) Effects of genic substitution at the agouti, brown, albino, dilute, and pink-eyed dilution loci on the proliferation and differentiation of mouse epidermal melanocytes in serum-free culture. Eur J Cell Biol 75: 184–191
Hirobe T, Kawa Y, Mizoguchi M, Ito S, Wakamatsu K (2002a) Effects of genic substitution at the pink-eyed dilution locus on the proliferation and differentiation of mouse epidermal melanocytes in vivo and in vitro. J Exp Zool 292: 351–366
Hirobe T, Wakamatsu K, Ito S, Abe H, Kawa Y, Mizoguchi M (2002b) Stimulation of the proliferation and differentiation of mouse pink-eyed dilution epidermal melanocytes by excess tyrosine in serum-free primary culture. J Cell Physiol 191: 162–172
Hirobe T, Wakamatsu K, Ito S (2003a) Changes in the proliferation and differentiation of neonatal mouse pink-eyed dilution melanocytes in the presence of excess tyrosine. Pigment Cell Res 16: 619–628
Hirobe T, Osawa M, Nishikawa S-I (2003b) Steel factor controls the proliferation and differentiation of neonatal mouse epidermal melanocytes in culture. Pigment Cell Res 16: 644–655
Hirobe T, Furuya R, Ifuku O, Osawa M, Nishikawa S-I (2004a) Granulocyte-macrophage colony-stimulating factor is a keratinocyte-derived factor involved in regulating the proliferation and differentiation of neonatal mouse epidermal melanocytes in culture. Exp Cell Res 297: 593–606
Hirobe T, Osawa M, Nishikawa S-I (2004b) Hepatocyte growth factor controls the proliferation of cultured epidermal melanoblasts and melanocytes from newborn mice. Pigment Cell Res 17: 51–61
Hirobe T, Abe H, Wakamatsu K, Ito S, Kawa Y, Soma Y, Mizoguchi M (2007) Excess tyrosine rescues the reduced activity of proliferation and differentiation of cultured recessive yellow melanocytes derived from neonatal mouse epidermis. Eur J Cell Biol 86: 315–330
Imokawa G, Mishima Y (1981) Isolation and biochemical characterization of tyrosinase-rich GERL and coated vesicle in melanin synthesizing cells. Brit J Dermatol 104: 169–178
Imokawa G, Yada Y, Miyagishi M (1992) Endothelins secreted from human keratinocytes are intrinsic mitogens for human melanocytes. J Biol Chem 267: 24675–24680
Imokawa G, Yada Y, Kimura M, Morisaki N (1996) Granulocyte/macrophage colony-stimulating factor is an intrinsic keratinocyte-derived growth factor for human melanocytes in UVA-induced melanosis. Biochem J 313: 625–631
Imokawa G, Kobayashi T, Miyagishi M, Higashi K, Yada Y (1997) The role of endothelin-1 in epidermal hyperpigmentation and signaling mechanisms of mitogenesis and melanogenesis. Pigment Cell Res 10: 218–228
Ito S (2003) A chemist's view of melanogenesis. Pigment Cell Res 16: 230–236
Kunisada T, Yoshida H, Yamazaki H, Miyamoto A, Hemmi H, Nishimura E, Shultz LD, Nishikawa S-I, Hayashi S-I (1998) Transgene expression of steel factor in the basal layer of epidermis promotes survival, proliferation, differentiation and migration of melanocyte precursors. Development 125: 2915–2923
Kunisada T, Yamazaki H, Hirobe T, Kamei S, Omoteno M, Tagaya H, Hemmi H, Koshimizu U, Nakamura T, Hayashi S-I (2000) Keratinocyte expression of transgenic hepatocyte growth factor affects melanocyte development, leading to dermal melanocytosis. Mech Dev 94: 67–78
Lamoreux ML, Zhou B-K, Rosemblat S, Orlow SJ (1995) The pinkeyed-dilution protein and the eumelanin/pheomelanin switch: in support of a unifying hypothesis. Pigment Cell Res 8: 263–270
Markert CL, Silvers WK (1956) The effects of genotype and cell environment on melanoblast differentiation in the house mouse. Genetics 41: 429–450
Maul GG (1969) Golgi-melanosome relationship in human melanoma *in vitro*. J Ultrastruct Res 26: 163–176
Mayer TC (1973) The migratory pathway of neural crest cells into the skin of mouse embryos. Dev Biol 34: 39–46
Mishima Y (1960) New technique for comprehensive demonstration of melanin, premelanin, and tyrosinase sites–combined dopa-premelanin reaction. J Invest Dermatol 34: 355–360
Moyer FH (1966) Genetic variations in the fine structure and ontogeny of mouse melanin granules. Am Zool 6: 43–66
Novikoff AB, Alabara A, Biempica L (1968) Ultrastructural and cytochemical observations on B-16 and Harding-Passey mouse melanomas. The origin of premelanosomes and compound melanosomes. J Histochem Cytochem 16: 299–319
Orlow SJ (1995) Melanosomes are specialized members of the lysosomal lineage of organelles. J Invest Dermatol 105: 3–7
Orlow SJ, Brilliant MH (1999) The pink-eyed dilution locus controls the biogenesis of melanosomes and levels of melanosomal proteins in the eye. Exp Eye Res 68: 147–154
Ozeki H, Ito S, Wakamatsu K, Hirobe T (1995) Chemical characterization of hair melanins in various coat-color mutants of mice. J Invest Dermatol 105: 361–364
Prota G (1980) Recent advances in the chemistry of melanogenesis in mammals. J Invest Dermatol 75: 122–127
Puri N, Gardner JM, Brilliant MH (2000) Aberrant pH of melanosomes in pink-eyed dilution (*p*) mutant melanocytes. J Invest Dermatol 115: 607–613
Rawles ME (1947) Origin of pigment cells from the neural crest in the mouse embryo. Physiol Zool 20: 248–266
Rinchik EM, Bultman SJ, Horsthemke B, Lee S-T, Strunk KM, Spritz RA, Avidano KM, Jong MTC, Nicholls RD (1993) A gene for the mouse pink-eyed dilution locus and for human type II oculocutaneous albinism. Nature 361: 72–76
Rosemblat S, Durham-Pierre D, Gardner JM, Nakatsu Y, Brilliant MH, Orlow SJ (1994) Identification of a melanosomal membrane protein encoded by the pink-eyed dilution (type II oculo-

cutaneous albinism) gene. Proc Natl Acad Sci USA 91: 12071–12075

Rosemblat S, Sviderskaya EV, Easty DJ, Wilson A, Kwon BS, Bennett DC, Orlow SJ (1998) Melanosomal defects in melanocytes from mice lacking expression of the pink-eyed dilution gene: correction by culture in the presence of excess tyrosine. Exp Cell Res 239: 344–352

Russell ES (1949) A quantitative histological study of the pigment found in the coat-color mutants of the house mouse. IV. The nature of the effects of genic substitution in five major allelic series. Genetics 34: 146–166

Seiji M, Shimao K, Birbeck MSC, Fitzpatrick TB (1963) Subcellular localization of melanin biosynthesis. Ann NY Acad Sci 100: 497–533

Sidman RL, Pearlstein R (1965) Pink-eyed dilution (*p*) gene in rodents: increased pigmentation in tissue culture. Dev Biol 12: 93–116

Silvers WK (1979) The Coat Colors of Mice. Springer-Verlag, Berlin

Slominski A, Jastreboff P, Pawelek J (1989) L-tyrosine stimulates induction of tyrosinase activity by MSH and reduces cooperative interactions between MSH receptors in hamster melanoma cells. Biosci Rep 9: 579–586

Staleva L, Manga P, Orlow SJ (2002) Pink-eyed dilution protein modulates arsenic sensitivity and intracellular glutathione metabolism. Mol Biol Cell 13: 4206–4220

Tamate HB, Hirobe T, Wakamatsu K, Ito S, Shibahara S, Ishikawa K (1989) Levels of tyrosinase and its mRNA in coat-color mutants of C57BL/10J congenic mice: effects of genic substitution at the agouti, brown, albino, dilute, and pink-eyed dilution loci. J Exp Zool 250: 304–311

Thody AJ, Ridley K, Penny RJ, Chalmers R, Fisher C, Shuster S (1983) MSH peptides are present in mammalian skin. Peptides 4: 813–816

Toyofuku K, Valencia JC, Kushimoto T, Costin G-E, Virador VM, Viera WD, Ferrans VJ, Hearing VJ (2002) The etiology of oculocutaneous albinism (OCA) type II: the pink protein modulates the processing and transport of tyrosinase. Pigment Cell Res 15: 217–224

Wakamatsu K, Hirobe T, Ito S (2007) High levels of melanin-related metabolites in plasma from pink-eyed dilution mice. Pigment Cell Res 20: 222–224

Yaar M, Grossman K, Eller M, Gilchrest BA (1991) Evidence for nerve growth factor-mediated paracrine effects in human epidermis. J Cell Biol 115: 821–828

Yada Y, Higuchi K, Imokawa G (1991) Effects of endothelins on signal transduction and proliferation in human melanocytes. J Biol Chem 266: 18352–18357

Yohn JJ, Morelli JG, Walchak SJ, Rundell KB, Norris DA, Zamora MR (1993) Cultured human keratinocytes synthesize and secrete endothelin-1. J Invest Dermatol 100: 23–26

(Received May 27, 2008 / Accepted August 5, 2008)